HHS Public Access

Author manuscript

J Proteome Res. Author manuscript; available in PMC 2020 June 07.

Published in final edited form as:

J Proteome Res. 2019 June 07; 18(6): 2624–2631. doi:10.1021/acs.jproteome.9b00134.

Quantitative Interrogation of the Human Kinome Perturbed by Two BRAF Inhibitors

Weili Miao[†], **Yinsheng Wang**[*,†]

[†]Department of Chemistry, University of California, Riverside, California 92521-0403, United States

Abstract

Oncogenic BRAF mutations contribute to the development of a number of cancers, and small-molecule BRAF inhibitors have been approved by the Food and Drug Administration (FDA) for anticancer therapy. In this study, we employed two targeted quantitative proteomics approaches for monitoring separately the alterations in protein expression and ATP binding affinities of kinases in cultured human melanoma cells elicited by two FDA-approved small-molecule BRAF inhibitors, dabrafenib and vemurafenib. Our results showed that treatment with the two inhibitors led to markedly different reprograming of the human kinome. Furthermore, we confirmed that vemurafenib could compromise the ATP binding capacity of MAP2K5 *in vitro* and inhibit its kinase activity in cells. Together, our targeted quantitative proteomic methods revealed profound changes in expression levels of kinase proteins in cultured melanoma cells upon treatment with clinically used BRAF inhibitors and led to the discovery of novel putative target kinases for these inhibitors.

Graphical Abstract

[*]**Corresponding Author:** Tel.: (951)827-2700. yinsheng.wang@ucr.edu.

Supporting Information

The Supporting Information is available free of charge on the ACS Publications website at DOI: 10.1021/acs.jproteome.9b00134.

Additional figures as described in the text (PDF)

Relative protein expression levels and ATP-binding affinities of kinases in M14 cells with or without dabrafenib or vemurafenib treatment (XLSX)

Differential ATP binding affinities of kinase proteins in lysate of M14 cells with and without a 2-h incubation with 100 nM vemurafenib (XLSX)

The authors declare no competing financial interest.

All the raw files for LC-PRM and LC-MRM analyses of kinases were deposited into PeptideAtlas with the identifier number of PASS01178 (http://www.peptideatlas.org/PASS/PASS01178).

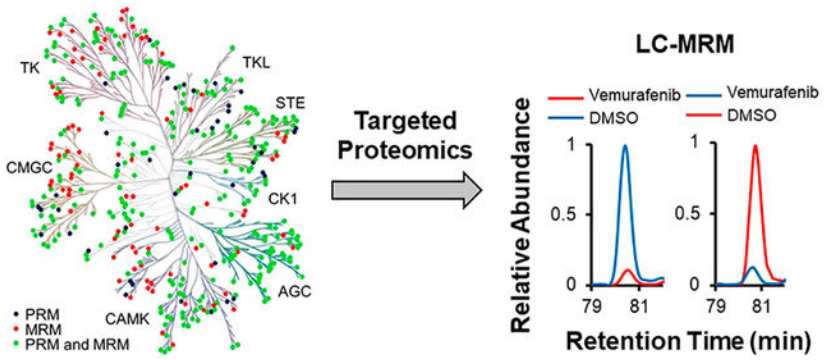

Keywords

quantitative proteomics; parallel-reaction monitoring; multiple-reaction monitoring; targeted proteomics; SILAC; kinase; kinase inhibitors; kinome; BRAF; melanoma

INTRODUCTION

BRAF is a serine/threonine-protein kinase that is involved in the mitogen-activated protein kinase (MAPK) signaling pathway that culminates in the activations of transcription factors important for cell growth, proliferation, and survival.[1] Oncogenic BRAF mutations are among the most frequently observed mutations in human cancer, especially melanoma.[2] The most common genotype is V600E (valine to glutamic acid),[3] with recent reports suggesting that this mutation accounts for up to 90% of BRAF mutant melanoma.[4] Thus, small-molecule BRAF inhibitors, including vemurafenib and dabrafenib, have been approved by the Food and Drug Administration (FDA) for the treatment of metastatic melanomas harboring the V600E mutant BRAF.[5,6] Although the response rate toward the inhibitors is high, most patients relapse at 6–8 months after therapy.[7]

Appropriate applications of these BRAF inhibitors in cancer chemotherapy require the knowledge about whether other kinases are also targeted by these inhibitors. The BRAF inhibitors are designed to disrupt directly the ATP-binding capabilities of BRAF.[8] However, the ATP-binding domains are highly conserved in kinases;[8,9] hence, compound selectivity is an important issue in the development of new kinase inhibitors.[10] Despite substantial efforts in optimizing the structures of BRAF inhibitors for selective binding toward BRAF, the inhibitors may also interact with the ATP binding pockets of other kinases.[11–13] In addition, cancer cells may respond to inhibitor treatment by altering the protein expression levels of kinases.[14] The knowledge about kinome reprogramming evoked by BRAF inhibitors and about their off-targets is, therefore, important for understanding more thoroughly the mechanisms through which these inhibitors confer therapeutic efficacy, side effects, and resistance.

In this study, we applied two targeted quantitative proteomic approaches for monitoring separately the changes in protein expression and ATP-binding affinities of ~80% of non-redundant kinases in M14 cells,[15–20] which carry the oncogenic V600E mutation,[21] upon treatment with two FDA-approved BRAF inhibitors, dabrafenib and vemurafenib. Our

results confirmed previously reported kinase targets for these inhibitors, uncovered many novel putative targets, and revealed profound changes in expression levels of kinase proteins in melanoma cells upon treatment with these BRAF inhibitors.

EXPERIMENTAL PROCEDURES

Cell Culture

WM-266–4 (ATCC), IGR-37 (obtained from Prof. Peter H. Duesberg),[22] M14 (National Cancer Institute) cells were cultured in Dulbecco's modified eagle medium (DMEM). All culture media were supplemented with 10% fetal bovine serum (Invitrogen, Carlsbad, CA) and penicillin (100 IU/mL). The cells were incubated at 37 °C in a humidified atmosphere containing 5% CO_2. Approximately 2×10^7 cells were harvested, washed with ice-cold PBS for three times, and lysed by incubating on ice for 30 min with CelLytic M (Sigma) cell lysis reagent containing 1% protease inhibitor cocktail. The cell lysates were centrifuged at 9000g at 4 °C for 30 min, and the resulting supernatants were collected. For SILAC experiments,[23] M14 cells were cultured in a medium containing unlabeled lysine and arginine, or [$^{13}C_6$, $^{15}N_2$]-lysine and [$^{13}C_6$]-arginine for at least 2 weeks to promote complete incorporation of the stable isotope-labeled amino acids.

Preparation of the Desthiobiotinylated Nucleotide Affinity Probe, and Desthiobiotin Labeling of ATP-Binding Proteins

The desthiobiotinylated nucleotide affinity probes were synthesized following previously published procedures.[24,25] Approximately 2×10^7 cells were harvested, washed for three times with ice-cold PBS, and lysed in a 1 mL lysis buffer, which contained 0.7% CHAPS, 50 mM HEPES (pH 7.4), 0.5 mM EDTA, 100 mM NaCl, and 10 μL (1:100) protease inhibitor cocktail on ice for 30 min. The cell lysates were centrifuged at 16000g at 4 °C for 30 min, and the supernatants were collected. Endogenous nucleotides in the resultant protein extract were removed by gel filtration using a NAP-5 column (Amersham Biosciences). Cell lysates were subsequently eluted into a buffer containing 50 mM HEPES (pH 7.4), 75 mM NaCl, and 5% glycerol. The amounts of proteins in the lysates were quantified using Quick Start Bradford Protein Assay (Bio-Rad). Prior to the labeling reaction, $MgCl_2$, $MnCl_2$, and $CaCl_2$ were added to the concentrated cell lysate until their final concentrations reached 50, 5, and 5 mM, respectively.

Tryptic Digestion of Protein Lysates

Cell lysates were washed with 8 M urea for protein denaturation, and dithiothreitol and iodoacetamide for cysteine reduction and alkylation, respectively. The proteins were subsequently digested with modified MS-grade trypsin (Pierce) at an enzyme/substrate ratio of 1:100 in 50 mM NH_4HCO_3 (pH 8.5) at 37 °C overnight. The resulting peptide mixture was dried in a Speed-vac, desalted with OMIX C18 pipet tips (Agilent Technologies), and analyzed by LC−MS and MS/MS on a Q Exactive Plus quadrupole-Orbitrap or a TSQ Vantage triple-quadrupole mass spectrometer (Thermo Fisher Scientific).

Sample Preparation, Multiple-Reaction Monitoring (MRM) and Parallel-Reaction Monitoring (PRM) Analyses

For assessing the alterations in ATP binding affinities of kinases in cultured cells induced by kinase inhibitors, we treated M14 cells with 100 nM dabrafenib or vemurafenib for 24 h. The cells were subsequently harvested by centrifugation and lysed, following the aforementioned procedures. The removal of endogenous nucleotides from protein lysate, labeling with desthiobiotin-conjugated ATP-affinity probe, tryptic digestion, and affinity purification of desthiobiotin-labeled peptides were conducted following the previously described procedures.[16] The resultant peptide mixture was subjected to LC−MS/MS analysis on a TSQ Vantage triple-quadrupole mass spectrometer, where the instrument was operated in the scheduled MRM mode and coupled with an Easy-nLC II system. The peptides were separated using a 130 min linear gradient of 2–35% acetonitrile in 0.1% formic acid and the flow rate was 230 nL/min. The spray voltage was 1.9 kV. Q1 and Q3 resolutions were 0.7 Da and the cycle time was 5 s.

To assess how vemurafenib modulates the ATP binding affinities of kinases in cell lysate, we removed endogenous nucleotides from the whole-cell protein lysate of M14 cells, and treated the resultant lysate (1 mg/mL) with 100 nM vemurafenib (or DMSO control) at room temperature for 2 h prior to labeling with desthiobiotin-conjugated ATP-affinity probe. The samples were then processed and subjected to LC−MRM analysis in the same way as described above.

To examine the differential expression of protein kinases in inhibitor-treated cells, we conducted both forward and reverse SILAC labeling experiments. In this context, the lysates of light-labeled, inhibitor-treated cells and heavy-labeled, mock-treated (with DMSO) cells were combined at 1:1 ratio (by mass) in the forward SILAC experiments, whereas the reverse SILAC experiments were performed in the opposite way. The whole-cell protein lysates were subsequently digested following the above-described procedures, and the resulting peptides were analyzed on a Q Exactive Plus quadrupole-Orbitrap mass spectrometer in the scheduled PRM mode. The mass spectrometer was coupled with an EASY-nLC 1200 system, and the samples were automatically loaded onto a 4 cm trapping column (150 μm i.d.) packed with ReproSil-Pur 120 C18-AQ resin (5 μm in particle size and 120 Å in pore size, Dr. Maisch GmbH HPLC) at 3 μL/min. The trapping column was coupled to a 20 cm fused silica analytical column (PicoTip Emitter, New Objective, 75 μm i.d.) packed with ReproSil-Pur 120 C18-AQ resin (3 μm in particle size and 120 Å in pore size, Dr. Maisch GmbH HPLC). The peptides were then separated using a 140 min linear gradient of 9–38% acetonitrile in 0.1% formic acid and at a flow rate of 300 nL/min. The spray voltage was 1.8 kV.

The linear predictor of empirical RT from iRT[26] for targeted kinase peptides was determined by the linear regression of RT vs iRT of tryptic peptides of BSA obtained for the chromatography setup prior to the analysis of kinase peptides.[16,27,28] This RT-iRT linear relationship was redetermined in every eight LC-PRM runs by injecting another BSA tryptic digestion mixture. The targeted precursor ions were monitored in eight separate injections for each sample in scheduled PRM mode with an 8 min retention time window. The

precursor ions of tryptic peptides from kinase proteins were isolated and collisionally activated in the HCD cell at a collision energy of 27.

All raw data acquired from LC-MRM and LC-PRM analyses were processed using Skyline (version 3.5)[29] for the generation of extracted-ion chromatograms and for peak integration. The targeted peptides were first manually checked to ensure the overlaid chromatographic profiles of multiple fragment ions derived from light and heavy forms of the same peptide. The data were then analyzed to confirm that the distribution of the relative intensities of multiple transitions for the same precursor ion is correlated with the theoretical distribution in the kinome MS/MS spectral library. The sum of peak areas from all transitions of light or from heavy forms of peptides was used for quantification.

Western Blot

WM-266–4, IGR-37, M14 cells were cultured in a 6-well plate and the cells were lysed at 40–50% confluency following the above-described procedures. For Western blot analysis of p-ERK5, the cells were treated with 100 ng/mL FGF21 (Sigma-Aldrich) for 20 min and then harvested for cell lysis. The concentrations of proteins in the resulting lysates were determined by using the Bradford Assay (Bio-Rad), and 10 μg protein lysate was denatured by boiling in Laemmli loading buffer and resolved by SDS-PAGE. The proteins were subsequently transferred onto a nitrocellulose membrane at 4 °C overnight. The resulting membrane was blocked with PBS-T (PBS with 0.1% Tween 20) containing 5% milk (Bio-Rad) at 4 °C for 6 h. The membrane was then incubated with primary antibody at 4 °C overnight and subsequently with secondary antibody at room temperature for 1 h. After the membrane was thoroughly washed with PBS-T, the HRP signal was detected with Pierce ECL Western Blotting Substrate (Thermo).

Antibodies recognizing human AK1 (Santa Cruz Biotechnology, sc-165981, 1:1000 dilution), ARAF (Santa Cruz Biotechnology, sc-166771, 1:4000 dilution), BRAF (Santa Cruz Biotechnology, sc-5284, 1:4000 dilution), CHK1 (Cell Signaling Technology, 2360S, 1:2000 dilution), EGFR (Santa Cruz Biotechnology, sc-03, with a 1:10000 dilution), ERK5 (Santa Cruz Biotechnology, sc-393405, with a 1:1000 dilution), p-ERK5 (T218/Y220, Santa Cruz Biotechnology, sc-135761, with a 1:1000 dilution), IGF2R (Santa Cruz Biotechnology, sc-14408, 1:1000 dilution), JAK3 (Thermo Fishier Scientific, AHO1572, 1:1000 dilution), MAP3K5 (a.k.a. ASK1, Santa Cruz Biotechnology, sc-5294, 1:2000 dilution), MAP2K5 (a.k.a. MEK5, Santa Cruz Biotechnology, sc-365198, 1:2000 dilution), MAP3K3 (a.k.a. MEKK3, Santa Cruz Biotechnology, sc-136260, 1:1000 dilution), MEK1 (Santa Cruz Biotechnology, sc-6250, 1:2000 dilution), p-MEK1 (Santa Cruz Biotechnology, sc-136542, 1:1000 dilution), mTOR (Cell Signaling Technology, 2972S, 1:1000 dilution), and STK26 (Abcam, ab52491, 1:20000 dilution) were employed as primary antibodies. Horseradish peroxidase-conjugated antirabbit IgG, IRDye 680LT Goat anti-Mouse IgG and donkey antigoat IgG-HRP (Santa Cruz Biotechnology, sc-2020, 1:10000 dilution) were used as secondary antibodies. Membranes were also probed with β-actin antibody (Cell Signaling #4967, 1:10000 dilution) to confirm equal protein loading.

RESULTS AND DISCUSSION

Profound Alterations in Kinase Protein Expression in M14 Human Melanoma Cells upon Treatment with BRAF Inhibitors

We employed our recently reported scheduled LC-PRM analysis[19] together with metabolic labeling using SILAC (Figure 1a)[23] to assess the reprogramming of the human kinome in M14 cells induced by two BRAF inhibitors. The M14 cells were chosen because they carry the frequently observed BRAF V600E mutation.[21]

The results from the PRM-based targeted proteomic method yielded quantitative results for 302 and 289 unique kinases in M14 cells treated with dabrafenib and vemurafenib, respectively (Table S1). The same retention time and a dot product (dotp) value greater than 0.7 were shown for all PRM transitions (4–6 transitions) used in kinase peptide quantification (Figure S1).[30] In addition, forward and reverse SILAC labeling experiments yielded consistent trends for the quantified kinases (Figure 1b,c, Table S1) and the average relative standard deviation for kinase protein quantification was 13.3% (Table S1). We further validated, by using Western blot analyses, the expression levels of 11 quantified kinases (mTOR, IGF2R, JAK3, CHK1, AK1, STK26, ARAF, BRAF, MAP2K1, MAP3K3, and MAP3K5) in M14 cells with or without dabrafenib or vemurafenib treatment. The results demonstrated that the PRM method afforded robust quantifications of the protein expression levels of kinases (Figure 2).

While both dabrafenib and vemurafenib were intended to target the V600E and V600K mutants of BRAF, treatment of M14 melanoma cells with these two inhibitors led to markedly different reprograming of the human kinome (Figures 3 and 4a). Specifically, treatment with 100 nM dabrafenib led to the up- and down-regulations of 27 and 42 kinases, respectively (Figure 3a), whereas the corresponding treatment with vemurafenib resulted in the up- and down-regulations of 58 and 5 kinases, respectively (Figure 3b).

To explore further the attenuated expression of a large number of kinase proteins induced by dabrafenib, we performed a time-dependent experiment, where we treated M14 cells with 100 nM dabrafenib for shorter durations (i.e., 4 and 12 h) and examined, using the aforementioned LC-PRM method, the protein expression levels of kinases at these two time points. Our result showed that many kinases exhibited augmented protein expression at 4 h following dabrafenib treatment and some kinases started to display diminished expression after 12 h (Figure S2, Table S1), suggesting that the decreased expression of most kinases occurred after 12 h of dabrafenib exposure (Figure S2, Table S1).

Alterations in ATP Binding Affinities of Kinases Elicited by BRAF Inhibitors

We further examined the changes in ATP binding affinities of kinases in cultured human cells following treatment with these BRAF inhibitors. Labeling with isotope-coded ATP affinity probes, in conjunction with LC−MS/MS analysis in the MRM mode, was found to afford a high-throughput and highly sensitive assessment about the ATP binding affinities of kinases in cultured human cells (Figure S3).[15,16] In this respect, the ratio for a kinase (in inhibitor-treated over DMSO-treated cells) obtained from labeling with ATP affinity probe

and LC−MRM is influenced by both the protein expression level and the ATP binding affinity of the kinase.[31]

We next applied the MRM-based method to assess the perturbations in ATP binding affinities of kinases (Figure S3) upon treatment with the two FDA-approved small-molecule BRAF inhibitors. We found that the ATP binding affinities of 38 and 9 kinases in M14 cells were attenuated following exposure to dabrafenib and vemurafenib, respectively (ratio <0.67, Table S1, Figures S4). In particular, our results confirmed BRAF as a target kinase for both dabrafenib and vemurafenib (Figure 4b,c, Table S1). In addition, ARAF, which was previously identified as a direct target of dabrafenib,[11,32] was detected with the ATP binding affinity being attenuated by more than 40% (Figure 4b, Figure S4, and Table S1). In keeping with previous findings,[33,34] we observed that vemurafenib exposure resulted in reduced ATP binding affinities of ARAF, BRAF, and ZAK (Figure S4, Table S1). Our capability in identifying previously reported target kinases for these BRAF inhibitors underscored that our quantitative proteomic strategy is effective in uncovering potential kinase targets for small-molecule kinase inhibitors.

Aside from discovering that those kinases exhibited reduced ATP binding affinities upon inhibitor treatment, we were able to detect 18 kinases displaying augmented binding affinities toward ATP upon treatments with dabrafenib or vemurafenib (i.e., with ratio greater than 1.5. Figure S4, Table S1). Among these kinases, CRAF is known to be activated by dabrafenib via a paradoxical pathway through the drug-mediated inhibition of one protomer of BRAF in the BRAF-CRAF heterodimer.[34]

Vemurafenib Suppresses the ATP-Binding Affinity of MAP2K5

In addition to ARAF, BRAF, and ZAK (Figure 4 and Figure S4), our results showed that vemurafenib treatment led to the diminished ATP binding affinities of several other kinases, including MAP2K5 (Figure 5a–c). In this vein, the inhibition of MAP2K5 by vemurafenib is even more pronounced than that of BRAF (Figure 5a), and similar inhibition of MAP2K5 was previously observed for PLX-4720, another BRAF inhibitor and a structural analogue of vemurafenib.[35] In agreement with the proteomic data, results from Western blot analysis showed that treatment of WM-266–4, IGR-37 and M14 cells with vemurafenib led to a marked diminution in the kinase activity of MAP2K5 (as reflected by reduced p-ERK5), albeit with no appreciable change in protein expression level of MAP2K5 (Figure 5b,c, and Figure S5). However, the proliferation of the M14 cells was not inhibited upon treatment with up to 1 μM BIX-02188, a small-molecule inhibitor for MAP2K5 (Figure S6). Thus, inhibition of MAP2K5 does not constitute a major mechanism for the cytotoxic effects of vemurafenib in BRAF-V600E mutant melanoma cells.

For comparison, we also examined the changes in ATP binding affinities of kinases in the whole-cell lysate of M14 cells upon treatment with vemurafenib (Figure S7). We were able to quantify 268 kinases, among which 7 exhibited reduced ATP binding affinities after 100 nM vemurafenib treatment (Figure S8, Table S2). Among these kinases, ARAF, ZAK, and MAP2K5 exhibited markedly lower ATP binding affinities in the lysate treated with vemurafenib (Figure 5d,e and Figure S8). In addition, the *in vitro* assay with the use of cell lysate provides information about other kinases exhibiting lower ATP binding affinities upon

treatment with 100 nM vemurafenib, including SRC (Figure 5f), IP6K1, FER, and PRPS1, whereas these four kinases did not display reduced ATP binding affinities in the above cell-based experiments. On the other hand, AK6, ABR, BRAF, CHUK, FGFR3, and PEAK1 displayed reduced ATP binding affinities in cellular experiments; however, all of them except CHUK1 were not detected in the *in vitro* assay. The failure to detect these five kinases could be attributed to the lack of stability of these kinases, where the *in vitro* experiment involved a 2-h incubation of the lysate with vemurafenib prior to ATP affinity probe labeling. The differences in vemurafenib-elicited variations in ATP binding affinities, as revealed from the *in cellulo* and *in vitro* assays, could arise from the presence of transient and unstable protein-protein interactions that may modulate the kinase's capability in binding to ATP.

CONCLUSIONS

In this study, we employed two targeted proteomic approaches to explore the alterations in protein expression and ATP binding affinity of kinases in cultured human cells upon treatment with two FDA-approved BRAF inhibitors. We were able to quantify the perturbations in protein expression levels and ATP binding affinities of approximately 300 kinases in BRAF V600E-carrying M14 human melanoma cells upon exposure to each BRAF inhibitor by employing LC−PRM analysis of the tryptic digestion mixture of whole cell lysate and ATP-affinity probe pull-down coupled with LC−MRM analysis, respectively. We observed that, whereas treatment with vemurafenib stimulated the expression of a large number of kinases, exposure to dabrafenib led to diminished protein expression of a large number of kinases. In addition, the ATP binding affinity of MAP2K5 is inhibited by vemurafenib in both *in cellulo* and *in vitro* experiments, suggesting MAP2K5 is a novel binding target for vemurafenib. Consistent with the results obtained from quantitative proteomic analyses, Western blot analysis revealed that exposure of M14 cells to vemurafenib led to diminished phosphorylation of ERK5.

The results from the present study, together with our recent work on imatinib,[19] demonstrate that the two quantitative proteomic methods constitute powerful approaches for revealing, at the proteome-wide scale, the alterations in protein expression and ATP binding affinities of kinases. In this regard, it is also worth discussing the limitations of the study. In particular, our quantitative proteomic experiments for ATP binding affinity assessment were conducted by using a single concentration of the ATP acyl nucleotide probe (i.e., 100 μM) and BRAF inhibitor (i.e., 100 nM). Our underlying assumption is that, under such conditions, the ATP acyl nucleotide probe would compete directly with BRAF inhibitors for binding to ATP binding pocket of kinases. On the grounds that the concentrations of kinases in cells can vary by several orders of magnitude, this assumption may not be valid for some kinases whose expression levels far exceed 100 nM. Thus, it will be important to examine, in the future, how the ATP affinity probe labeling efficiencies can be altered with the use of different concentrations of kinase inhibitors.

Supplementary Material

Refer to Web version on PubMed Central for supplementary material.

ACKNOWLEDGMENTS

This work was supported by the National Institutes of Health (R01 CA210072).

REFERENCES

(1). McCain J The MAPK (ERK) Pathway: Investigational Combinations for the Treatment Of BRAF-Mutated Metastatic Melanoma. P. T 2013, 38, 96–108. [PubMed: 23599677]

(2). RAhman M; Smith R; Salajegheh A; Lam A BRAF inhibitor therapy for melanoma, thyroid and colorectal cancers: development of resistance and future prospects. Curr. Cancer Drug Targets 2014, 14, 128–143. [PubMed: 24446739]

(3). Davies H; Bignell GR; Cox C; Stephens P; Edkins S; Clegg S; Teague J; Woffendin H; Garnett MJ; Bottomley W; Davis N; Dicks E; Ewing R; Floyd Y; Gray K; Hall S; Hawes R; Hughes J; Kosmidou V; Menzies A; Mould C; Parker A; Stevens C; Watt S; Hooper S; Wilson R; Jayatilake H; Gusterson BA; Cooper C; Shipley J; Hargrave D; Pritchard-Jones K; Maitland N; Chenevix-Trench G; Riggins GJ; Bigner DD; Palmieri G; Cossu A; Flanagan A; Nicholson A; Ho JWC; Leung SY; Yuen ST; Weber BL; Seigler HF; Darrow TL; Paterson H; Marais R; Marshall CJ; Wooster R; Stratton MR; Futreal PA Mutations utations of the BRAF gene in human cancer. Nature 2002, 417, 949–954. [PubMed: 12068308]

(4). Bradish JR; Cheng L Molecular pathology of malignant melanoma: changing the clinical practice paradigm toward a personalized approach. Hum. Pathol 2014, 45, 1315–1326. [PubMed: 24856851]

(5). Bollag G; Tsai J; Zhang J; Zhang C; Ibrahim P; Nolop K; Hirth P Vemurafenib: the first drug approved for BRAF-mutant cancer. Nat. Rev. Drug Discovery 2012, 11, 873–886. [PubMed: 23060265]

(6). Menzies AM; Long GV Dabrafenib and trametinib, alone and in combination for *BRAF*-mutant metastatic melanoma. Clin. Cancer Res. 2014, 20, 2035–2043. [PubMed: 24583796]

(7). Chapman PB; Hauschild A; Robert C; Haanen JB; Ascierto P; Larkin J; Dummer R; Garbe C; Testori A; Maio M; Hogg D; Lorigan P; Lebbe C; Jouary T; Schadendorf D; Ribas A; O'Day SJ; Sosman JA; Kirkwood JM; Eggermont AMM; Dreno B; Nolop K; Li J; Nelson B; Hou J; Lee RJ; Flaherty KT; McArthur GA Improved survival with vemurafenib in melanoma with BRAF V600E mutation. N. Engl. J. Med 2011, 364, 2507–2516. [PubMed: 21639808]

(8). Wu P; Nielsen TE; Clausen MH FDA-approved small-molecule kinase inhibitors. Trends Pharmacol. Sci 2015, 36, 422–439. [PubMed: 25975227]

(9). Dancey J; Sausville EA Issues and progress with protein kinase inhibitors for cancer treatment. Nat. Rev. Drug Discovery 2003, 2, 296–313. [PubMed: 12669029]

(10). Bosc N; Meyer C; Bonnet P The use of novel selectivity metrics in kinase research. BMC Bioinf 2017, 18, 17.

(11). Fabian MA; Biggs WH 3rd; Treiber DK; Atteridge CE; Azimioara MD; Benedetti MG; Carter TA; Ciceri P; Edeen PT; Floyd M; Ford JM; Galvin M; Gerlach JL; Grotzfeld RM; Herrgard S; Insko DE; Insko MA; Lai AG; Lelias JM; Mehta SA; Milanov ZV; Velasco AM; Wodicka LM; Patel HK; Zarrinkar PP; Lockhart DJ A small molecule-kinase interaction map for clinical kinase inhibitors. Nat. Biotechnol 2005, 23, 329–36. [PubMed: 15711537]

(12). Davis MI; Hunt JP; Herrgard S; Ciceri P; Wodicka LM; Pallares G; Hocker M; Treiber DK; Zarrinkar PP Comprehensive analysis of kinase inhibitor selectivity. Nat. Biotechnol 2011, 29, 1046–1051. [PubMed: 22037378]

(13). Klaeger S; Heinzlmeir S; Wilhelm M; Polzer H; Vick B; Koenig P-A; Reinecke M; Ruprecht B; Petzoldt S; Meng C; Zecha J; Reiter K; Qiao H; Helm D; Koch H; Schoof M; Canevari G; Casale E; Depaolini SR; Feuchtinger A; Wu Z; Schmidt T; Rueckert L; Becker W; Huenges J; Garz A-K; Gohlke B-O; Zolg DP; Kayser G; Vooder T; Preissner R; Hahne H; Tõnisson N; Kramer K; Götze K; Bassermann F; Schlegl J; Ehrlich H-C; Aiche S; Walch A; Greif PA; Schneider S; Felder ER; Ruland J; Médard G; Jeremias I; Spiekermann K; Kuster B The target landscape of clinical kinase drugs. Science 2017, 358, No. eaan4368.

(14). Duncan JS; Whittle MC; Nakamura K; Abell AN; Midland AA; Zawistowski JS; Johnson NL; Granger DA; Jordan NV; Darr DB; Usary J; Kuan PF; Smalley DM; Major B; He X; Hoadley KA; Zhou B; Sharpless NE; Perou CM; Kim WY; Gomez SM; Chen X; Jin J; Frye SV; Earp HS; Graves LM; Johnson GL Dynamic reprogramming of the kinome in response to targeted MEK inhibition in triple-negative breast cancer. Cell 2012, 149, 307–21. [PubMed: 22500798]

(15). Xiao Y; Guo L; Wang Y A targeted quantitative proteomics strategy for global kinome profiling of cancer cells and tissues. Mol. Cell. Proteomics 2014, 13, 1065–1075. [PubMed: 24520089]

(16). Miao W; Xiao Y; Guo L; Jiang X; Huang M; Wang Y A high-throughput targeted proteomic approach for comprehensive profiling of methylglyoxal-induced perturbations of the human kinome. Anal. Chem 2016, 88, 9773–9779. [PubMed: 27626823]

(17). Patricelli MP; Nomanbhoy TK; Wu J; Brown H; Zhou D; Zhang J; Jagannathan S; Aban A; Okerberg E; Herring C; Nordin B; Weissig H; Yang Q; Lee J-D; Gray NS; Kozarich JW In situ kinase profiling reveals functionally relevant properties of native kinases. Chem. Biol 2011, 18, 699–710. [PubMed: 21700206]

(18). Patricelli MP; Szardenings AK; Liyanage M; Nomanbhoy TK; Wu M; Weissig H; Aban A; Chun D; Tanner S; Kozarich JW Functional interrogation of the kinome using nucleotide acyl phosphates. Biochemistry 2007, 46, 350–358. [PubMed: 17209545]

(19). Miao W; Guo L; Wang Y Imatinib-Induced Changes in Protein Expression and ATP-Binding Affinities of Kinases in Chronic Myelocytic Leukemia Cells. Anal. Chem 2019, 91, 3209–3214. [PubMed: 30773012]

(20). Miao W; Wang Y, Targeted quantitative kinome analysis identifies PRPS2 as a promoter for colorectal cancer metastasis. J. Proteome Res. 2019, DOI: 10.1021/acs.jproteome.9b00119.

(21). Hou P; Liu D; Dong J; Xing M The BRAF(V600E) causes widespread alterations in gene methylation in the genome of melanoma cells. Cell Cycle 2012, 11, 286–295. [PubMed: 22189819]

(22). Bloomfield M; Duesberg P Inherent variability of cancer-specific aneuploidy generates metastases. Mol. Cytogenet 2016, 9, 90. [PubMed: 28018487]

(23). Ong S-E; Blagoev B; Kratchmarova I; Kristensen DB; Steen H; Pandey A; Mann M Stable isotope labeling by amino acids in cell culture, SILAC, as a simple and accurate approach to expression proteomics. Mol. Cell. Proteomics 2002, 1, 376–386. [PubMed: 12118079]

(24). Xiao Y; Guo L; Jiang X; Wang Y Proteome-wide discovery and characterizations of nucleotide-binding proteins with affinity-labeled chemical probes. Anal. Chem 2013, 85, 3198–206. [PubMed: 23413923]

(25). Xiao Y; Guo L; Wang Y Isotope-Coded ATP Probe for Quantitative Affinity Profiling of ATP-Binding Proteins. Anal. Chem 2013, 85, 7478–7486. [PubMed: 23841533]

(26). Escher C; Reiter L; MacLean B; Ossola R; Herzog F; Chilton J; MacCoss MJ; Rinner O Using iRT, a normalized retention time for more targeted measurement of peptides. Proteomics 2012, 12, 1111–1121. [PubMed: 22577012]

(27). Miao W; Li L; Wang Y A targeted proteomic approach for heat shock proteins reveals DNAJB4 as a suppressor for melanoma metastasis. Anal. Chem 2018, 90, 6835–6842. [PubMed: 29722524]

(28). Miao W; Li L; Wang Y Identification of helicase proteins as clients for HSP90. Anal. Chem 2018, 90, 11751–11755. [PubMed: 30247883]

(29). MacLean B; Tomazela DM; Shulman N; Chambers M; Finney GL; Frewen B; Kern R; Tabb DL; Liebler DC; MacCoss MJ Skyline: an open source document editor for creating and analyzing targeted proteomics experiments. Bioinformatics 2010, 26, 966–968. [PubMed: 20147306]

(30). de Graaf EL; Altelaar AF; van Breukelen B; Mohammed S; Heck AJ Improving SRM assay development: a global comparison between triple quadrupole, ion trap, and higher energy CID peptide fragmentation spectra. J. Proteome Res. 2011, 10, 4334–4341. [PubMed: 21726076]

(31). Cravatt BF; Wright AT; Kozarich JW Activity-based protein profiling: from enzyme chemistry to proteomic chemistry. Annu. Rev. Biochem 2008, 77, 383–414. [PubMed: 18366325]

(32). Peng S-B; Henry JR; Kaufman MD; Lu W-P; Smith BD; Vogeti S; Rutkoski TJ; Wise S; Chun L; Zhang Y; Van Horn RD; Yin T; Zhang X; Yadav V; Chen S-H; Gong X; Ma X; Webster Y; Buchanan S; Mochalkin I; Huber L; Kays L; Donoho GP; Walgren J; McCann D; Patel P; Conti

I; Plowman GD; Starling JJ; Flynn DL Inhibition of RAF Isoforms and Active Dimers by LY3009120 Leads to Anti-tumor Activities in RAS or BRAF Mutant Cancers. Cancer Cell 2015, 28, 384–398. [PubMed: 26343583]

(33). Vin H; Ojeda SS; Ching G; Leung ML; Chitsazzadeh V; Dwyer DW; Adelmann CH; Restrepo M; Richards KN; Stewart LR; Du L; Ferguson SB; Chakravarti D; Ehrenreiter K; Baccarini M; Ruggieri R; Curry JL; Kim KB; Ciurea AM; Duvic M; Prieto VG; Ullrich SE; Dalby KN; Flores ER; Tsai KY BRAF inhibitors suppress apoptosis through off-target inhibition of JNK signaling. eLife 2013, 2, No. e00969.

(34). Hatzivassiliou G; Song K; Yen I; Brandhuber BJ; Anderson DJ; Alvarado R; Ludlam MJC; Stokoe D; Gloor SL; Vigers G; Morales T; Aliagas I; Liu B; Sideris S; Hoeflich KP; Jaiswal BS; Seshagiri S; Koeppen H; Belvin M; Friedman LS; Malek S RAF inhibitors prime wild-type RAF to activate the MAPK pathway and enhance growth. Nature 2010, 464, 431. [PubMed: 20130576]

(35). Davis MI; Hunt JP; Herrgard S; Ciceri P; Wodicka LM; Pallares G; Hocker M; Treiber DK; Zarrinkar PP Comprehensive analysis of kinase inhibitor selectivity. Nat. Biotechnol 2011, 29, 1046. [PubMed: 22037378]

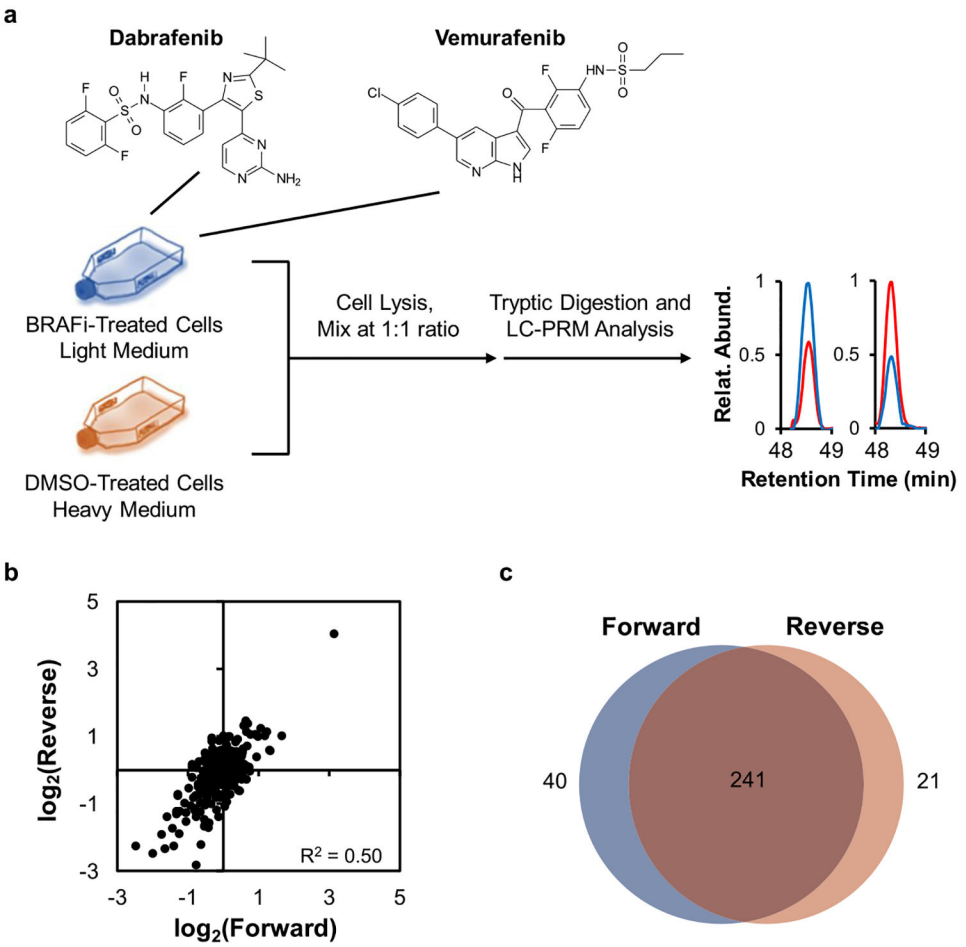

Figure 1.

PRM-based targeted proteomic approaches for interrogating the human kinome. (a) Experimental strategy for PRM-based targeted proteomic approaches. (b) A scatter plot displaying the correlation between the ratios obtained from forward and reverse SILAC labeling experiments in M14 cells with or without dabrafenib treatment. (c) A Venn diagram showing the overlap between quantified kinases from the forward and reverse SILAC labeling experiments in M14 cells with or without dabrafenib treatment.

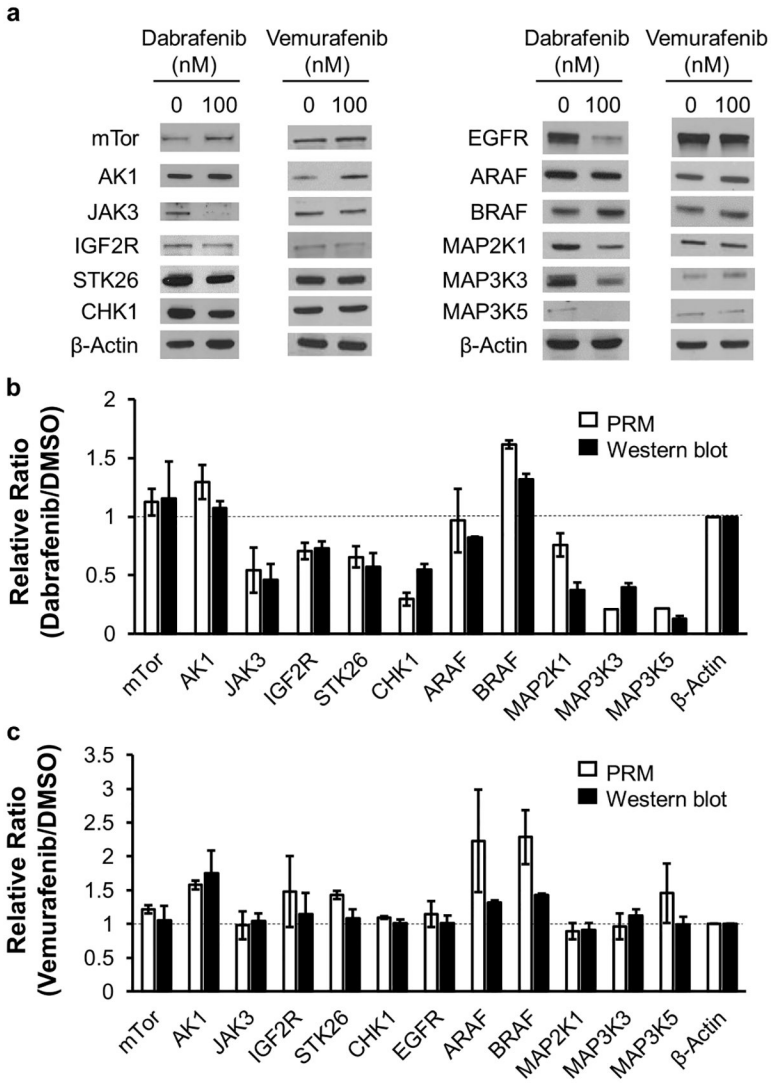

Figure 2.

Western blot analyses for validating the protein expression levels of kinases in M14 cells with or without dabrafenib/vemurafenib treatment. (a) Images from Western blot analyses of the expression levels of representative kinases in M14 cells with or without dabrafenib or vemurafenib treatment. The quantification results for the ratios of kinase proteins in dabrafenib- and vemurafenib-treated cells over control untreated cells are shown in panels b and c, respectively. The data represent the mean ± S.D. of the quantification results ($n = 3$).

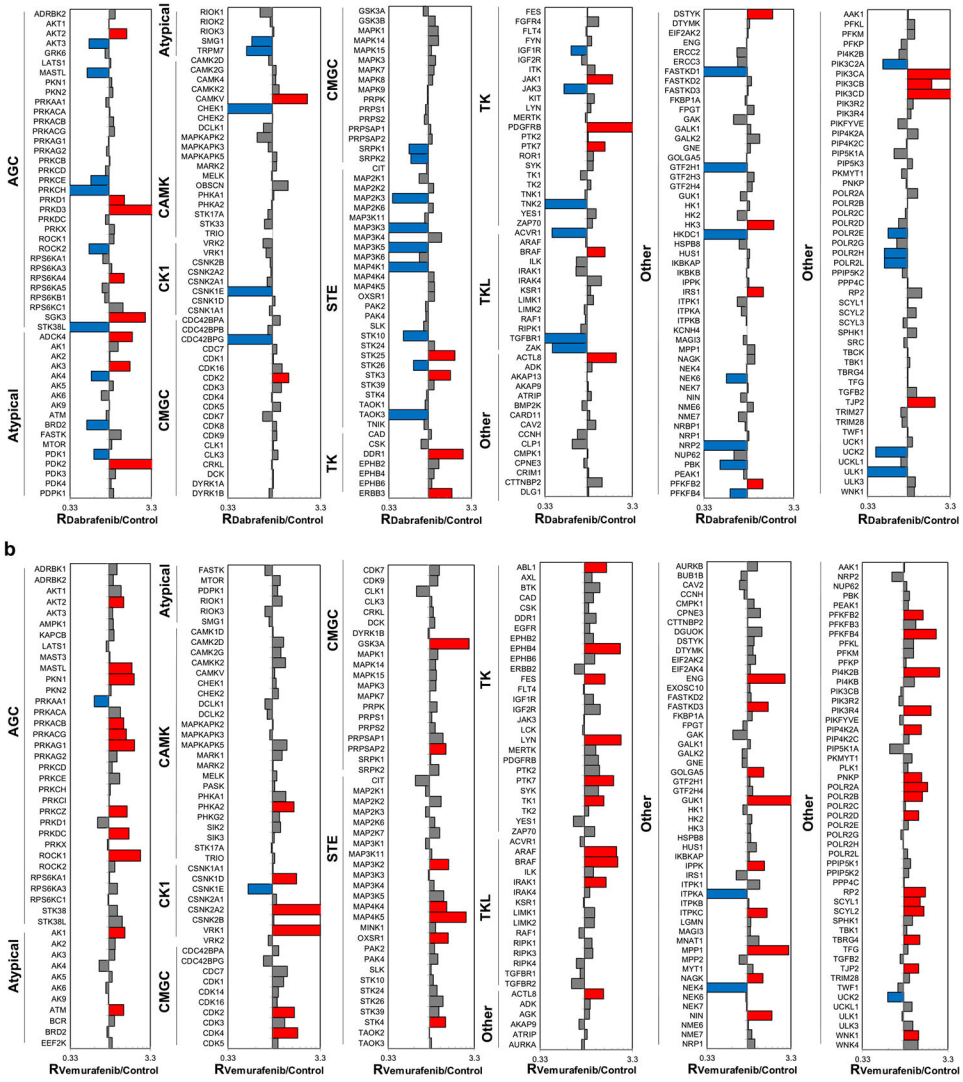

Figure 3.

Alterations in expression levels of kinase proteins in M14 cells after treatment with two small-molecule BRAF inhibitors, dabrafenib (a) and vemurafenib (b). The cells were treated with 100 nM inhibitor for 24 h. Displayed are the ratios of expression of kinase proteins in BRAF inhibitor-treated over mock (DMSO)-treated M14 cells, where the *X*-axis was plotted in $\log_{10}$ scale. The data represent the average ratios obtained from two forward and two reverse SILAC labeling experiments for dabrafenib treatment and two forward and one reverse SILAC labeling experiments for vemurafenib treatment. The red and blue bars designate those kinases that were up- and down-regulated, respectively, by at least 1.5-fold upon the inhibitor treatment (Table S1).

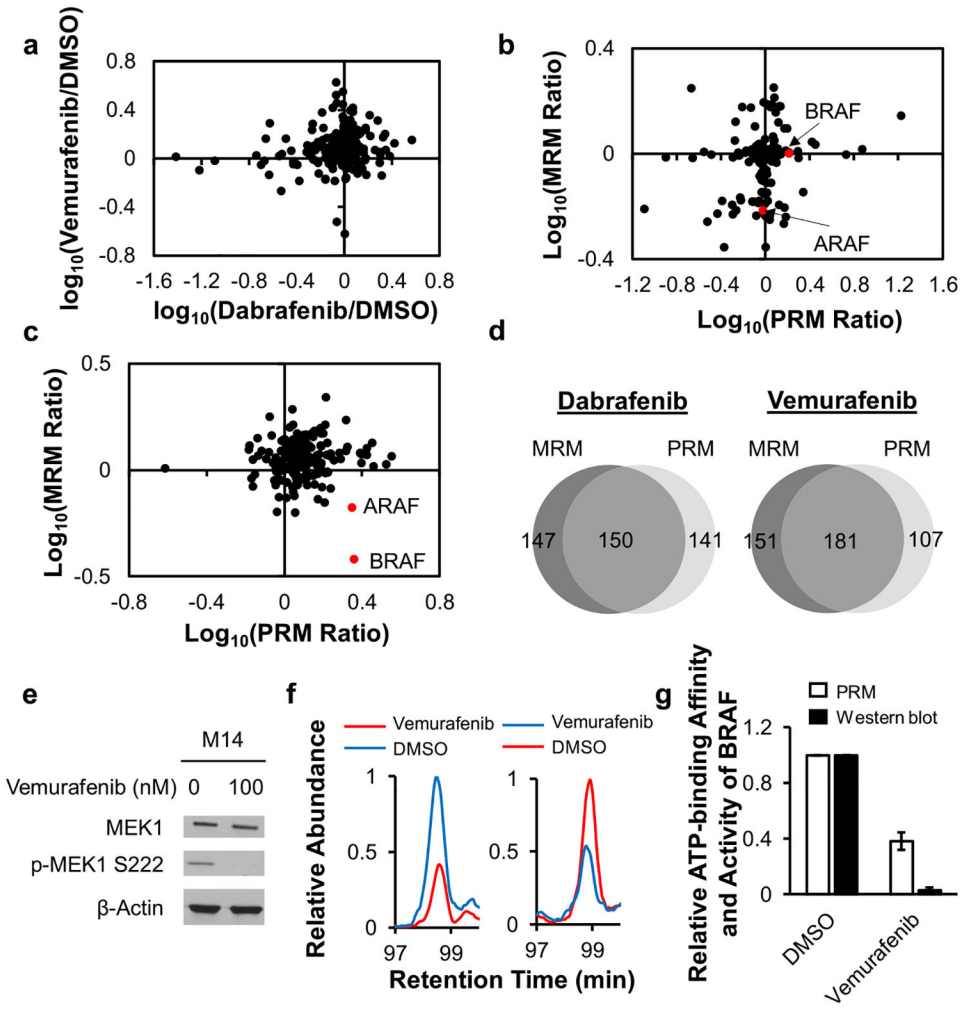

Figure 4.

PRM- and MRM-based targeted proteomic approaches for interrogating the perturbations in protein expression and ATP binding affinity of kinases induced by kinase inhibitor treatment. (a) A scatter plot showing the absence of apparent correlation of alterations in kinase protein expression triggered by dabrafenib and vemurafenib treatments. (b,c) Scatter plots showing the lack of correlation between the ratios of kinases in dabrafenib (b) and vemurafenib (c)-treated over control DMSO-treated cells obtained from the PRM and MRM methods. (d) Venn diagrams depicting the overlaps of the number of kinases that were quantified by the PRM- and MRM-based kinome profiling methods for cellular samples obtained from treatments with dabrafenib and vemurafenib. (e) Western blot for examining the expression and phosphorylation level of MEK1 protein. (f) MRM traces for a BRAF peptide modulated by vemurafenib treatment. (g) Quantitative comparison of ATP-binding affinity and activity of BRAF obtained from PRM and Western blot analyses, respectively. The data represent the mean ± S.D. of the quantification results ($n = 3$).

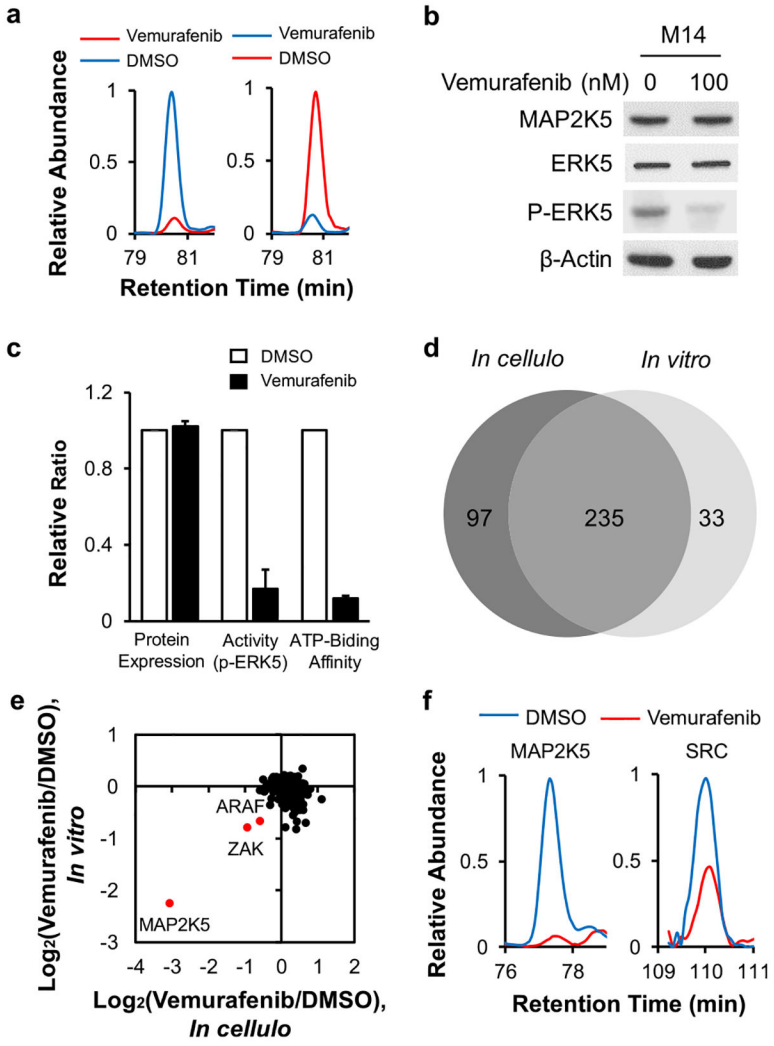

Figure 5.

Vemurafenib binds MAP2K5. (a) MRM traces for tryptic peptides of MAP2K5 in M14 cells with or without vemurafenib treatment. (b) Western blot for monitoring the expression levels of MAP2K5 and ERK5, and the phosphorylation level of ERK5. (c) Quantitative comparison of ratios of protein expression and activity of MAP2K5 obtained from Western blot analyses, and ATP-binding affinity obtained from MRM analyses. The data represent the mean ± S.D. of the quantification results ($n = 3$). (d) The Venn diagram showing the overlap between the cell-based and *in vitro* kinome profiling by vemurafenib treatment. (e) A scatter plot displaying the correlation between the ratios (vemurafenib treat/control) obtained from *in cellulo* (in M14 cells) and *in vitro* (M14 cell lysate) experiments, respectively. (f) MRM traces of MAP2K5 and SRC obtained from *in vitro* kinome profiling assay.